Наносистеми, наноматеріали, нанотехнології
Nanosistemi, Nanomateriali, Nanotehnologii
2026, т. 24, № 2, сс. 575–596
https://doi.org/10.15407/nnn.24.02.0575

PACS numbers: 68.37.Hk, 68.43.Jk, 68.43.Mn, 81.05.uj, 82.60.Hc, 82.60.Qr, 83.80.Mc

Preparation and Characterization of Nanocarbon Prepared from Thermal Cracking Residues of Sawdust

Hamid A. Salih, Saad F. Mahmood, and Mohmad M. Uonis

College of Science,
Department of New and Renewable Energy,
University of Mosul,
Mosul, Iraq

This study produces a new type of activated nanocarbon, using sawdust from woodworking shops in Mosul city, Iraq. The average particle size of this carbon produced is of 20–100 nm and is identified as nanocarbon. The drug chlorpheniramine is extracted from its aqueous solution. In this study, the Freundlich's and Langmuir's isotherms are used, where the Langmuir's model fits better the actual data of the analyzed system. This is evidenced by the results of high R^2 values of 0.9872 for Freundlich's model and 0.9935 for Langmuir's one. Thermodynamic analysis of equilibrium adsorption shows that it is a spontaneous process with negative ΔG^0 values and results in a regular increase (negative ΔS^0 value) after the adsorption process. In addition, physical adsorption forces ($\Delta H = -16.452$ kJ/mol) determine the bonding between the drug and the carbon surface, and the adsorption process results in a heat release. The three kinetic models are pseudo-first-order, pseudo-second-order, and implicit molecular diffusion. The results show that the equilibrium adsorption is followed by the pseudo-second-order reaction equation, and the adsorption process is governed by multiple mechanisms in addition to molecular-contact diffusion.

У цьому дослідженні було одержано новий тип активованого нановуглецю з використанням тирси з деревообробних цехів міста Мосул (Ірак). Середній розмір частинок цього одержаного вуглецю становить 20–100 нм і був ідентифікований як нановуглець. Препарат хлорфенірамін був екстраґований з його водного розчину. У цьому дослідженні використовувалися Фройндлішова та Ленґмюрова ізотерми, де Ленґмюрів модель краще відповідає фактичним даним стосовно аналізованої системи. Про це свідчать результати високих значень R^2: 0,9872 для Фройндлішового моделю та 0,9935 для Ленґмюрового моделю. Термодинамічна аналіза рівноважної адсорбції показує, що це є спонтанний процес з неґативними значеннями ΔG^0 і приводить до реґулярного збільшення (із неґативним значенням ΔS^0) після процесу адсорбції. Крім того, фізичні

сили адсорбції ($\Delta H = -16{,}452$ кДж/моль) визначають зв'язок між препаратом і поверхнею вуглецю, а процес адсорбції приводить до виділення тепла. Три кінетичні моделі були псевдопершого порядку, псевдодругого порядку та неявною молекулярною дифузією. Результати показують, що рівноважна адсорбція відповідає рівнянню реакції псевдодругого порядку, а процес адсорбції реґулюється кількома додатковими механізмами, окрім молекулярної контактної дифузії.

Key words: sawdust, nanocarbon, activated charcoal, eucalyptus trees, adsorption kinetic.

Ключові слова: тирса, нановуглець, активоване вугілля, евкаліпти, кінетика адсорбції.

(Received 16 October, 2024; in revised form, 21 November, 2024)

1. INTRODUCTION

One of the biggest problems in the modern world is environmental pollution, which is becoming more and more common due to industrial development and population growth. Industry is considered as one of the main sources of environmental pollution [1]. Chemical substances or their biodegradation products are pollutants, which affect aquatic ecology because they contain hazardous chemical groups [2]. However, besides its various uses in households, it is also vital for many economic impacts (*e.g.*, agriculture) and also has an impact on biological life (*e.g.*, water). One of the modern challenges and problems is the supply of drinking water to cities and other sectors. Rivers, lakes and groundwater can contribute. Due to the lack of water-treatment facilities, hospitals are forced to discharge heavy water into the main sewage network, which eventually flows into rivers [3].

The difficulty in treating these pollutants is that wastewater-treatment plants are unable to remove, reuse or, otherwise, utilize them that creates many problems and increases the amount of pollutants entering the river [4]. An antihistamine that enters into a river as a liquid pollutant is chlorpheniramine. Since it is one of the most prevalent environmental problems in the world, there is an urgent need to find a solution and solve it. Governments have begun to formulate regulations and laws regarding the location of laboratories and the treatment of water before it is discharged into the environment. So, researchers in this field develop low-cost adsorbent materials to combat various forms of pollution. Contaminated water and adsorbent materials can be treated by reactivating the materials, making them recyclable. Therefore, adsorption is one of the most direct methods to deal with pollution.

The most famous isotherm model that can be successfully applied to single-component systems is the Freundlich's equation. This model assumes that the surface of the adsorbent is not uniform due to the different energy levels of the adsorption sites, resulting in irregular potential energy on the surface. The value of the correlation coefficient (R^2) can be used to express the strength of the linear relationship and determine the extent, to which corresponding isotherm accurately represents the adsorption experimental data. This linear model can be expressed [5] as

$$\log q_e = \log K_F + n^{-1}\log C_e, \quad (1)$$

where K_F is the Freundlich's isotherm constant, q_e is an amount of adsorbed material per gram of adsorbent, which is known as the adsorption capacity at equilibrium [mg/g], C_e is a concentration of the remaining material, which is non-adsorbed at equilibrium [mg/L].

When plotting, the relationship between $\log q_e$ and $\log C_e$ gives a straight line with a slope of $1/n$ (as a measure of the strength of adsorption) and a cross section of $\log K_F$ (as a function of the adsorption capacity), while the value of n indicates the optimum value for achieving adsorption performance and the degree of non-openness of the adsorption performance layer: if it is only between 1–10, it means that the adsorption is good and is preferred, but, if n is less than 1, this adsorption is not preferred; when $n = 1$, this adsorption is linear, when $n < 1$, it is chemical adsorption, and when $n > 1$, it is physical adsorption [6].

The model assumes that molecules are adsorbed at a certain number of openings (pores) on the surface of a certain weight of adsorbent; these openings are energetically equivalent, each opening can only accommodate one adsorbed molecule, and the molecules adsorbed on the adsorbent surface do not interact with each other. Nor do they react with other attacking molecules present in the solution. Therefore, a monolayer of adsorbed molecules is formed on the adsorbent surface. According to the model, the adsorption phenomenon is initially rapid and then reaches equilibrium after the relative speeds are equal, due to the rate, at which molecules attach to the adsorbent surface and then return to the solution [7]. According to this model, the amount of adsorbed material is proportional to the part exposed to the adsorption phenomenon, while the number of returned particles is proportional to the part of the surface covered. The model can be expressed by the linear Eq. (2) [8]:

$$C_e/q_e = b^{-1}Q_{\max} + C_e/Q_{\max}, \quad (2)$$

where b is the constant of Langmuir's isotherm, $Q_{\max}$ is maximum

theoretical adsorption capacity of the adsorbent material, C_e and q_e are remaining concentration and adsorption capacity at equilibrium, respectively.

To obtain accurate information that explains the mechanism of adsorption and the kinetic forces affecting it, the following kinetic models were studied on the drug at issue.

Adsorption kinetics data were first described by Lagergren (1898), using a first-order equation, which is considered the first equation to describe adsorption rate based on capacity and has been used by many researchers since then. The first-order equation can be expressed as follows [9, 10]:

$$\ln(q_e - q_t) = \ln q_e - k_1 t. \tag{3}$$

In order to apply this model to actual adsorption data, a linear relationship must be established by plotting $\ln(q_e - q_t)$ *versus* time, and agreement must be achieved between the calculated and actual values of the adsorption capacity. This model is also used to describe the kinetics of adsorption, as this model explains, how the rate of speed depends on the adsorption capacity of the solid adsorbent and not on the concentration of the adsorbent. Unlike the other kinetic models, it predicts the behaviour of adsorption along the time period of adsorption. This is consistent with an adsorption mechanism that includes a step that determines the rate of speed, which may include countervailing forces through the sharing or exchange of electrons between the solution and the adsorbent, where the pseudo-second-order equation can be expressed as Eq. (4) [11]:

$$\frac{t}{q_t} = \frac{1}{k_2}(q_e)^2 + \frac{t}{q_e}. \tag{4}$$

In order to apply this model to practical adsorption data by plotting the relationship between t/q_t *versus* time t, it must give a linear relationship and a match must be obtained between the calculated and practical adsorption capacity value [12]. It is also possible to use the adsorption rate constant k_2 to find the value of the initial pseudo-second-order adsorption speed (h) through Eq. (5) [11]:

$$h = k_2(q_e)^2. \tag{5}$$

The overall rate of adsorption will be determined by the slowest step, which may be diffusion from the outer boundaries of the liquid to the adsorbent surface, or the implicit molecular diffusion within the pores of the adsorbent material. The rate of adsorption on the active sites is assumed to be fast, and one of the important things that must be found and determined is the potential rate spe-

cific to the adsorption mechanism. According to Morris–Weber [13], if the implicit molecular diffusion is the controlling factor depending on the reaction rate, the process of removing adsorbed materials changes with the square root of time. As a result, it is possible to calculate the rate of adsorption by calculating the adsorption capacity of the adsorbent as a function of the square root of time, as the implicit molecular diffusion model can be represented [14, 15] as

$$q_t = K_{diff} t^{1/2} + C, \tag{6}$$

where K_{diff} [mg/g·min$^{1/2}$] represents the rate constant for implicit molecular diffusion, while C [mg/g] is the value of the cross-section, and the value of K_{diff} can be found from the slope of the straight line.

The aim of the research is to produce activated carbon from available and inexpensive raw materials, estimate the adsorption capacity, determine the optimal conditions and study the adsorption kinetics and thermodynamics.

2. EXPERIMENTAL METHOD

2.1. Instruments

Various procedures and equipment were utilized to assess the materials, including: a UV–visible spectrophotometer (Shimadzu Corporation of Japan manufactured this two-track instrument (model 1800-UV)); sensitive electronic scale: model 200-CR, with four decimal places; drying oven used to dry the sawdust (model 3510); water bath shaker (model Bs-11, Jwrio Tech, made in S. Korea); centrifuge is used to separate samples (precipitates from solutions) and it is a German-made Hermle Z200A equipped by HERME LABORTECHNIK; SEM device (MIRA3LMU); thermal cracking device (pyrolysis) Silver Crust Type Household Grain Mill.

2.2. Chemical Materials

BDH-Fluka Company supplied all of the ingredients necessary, including hydrochloric acid, ethanol, potassium hydroxide, and distilled water, to synthesize activated carbon. A novel sort of charcoal was made from pyrolysis of ground sawdust, washing them multiple times, drying them under open air, and then placing them in an electric oven at 105–110°C for 48 hours. The initial carbonization process is carried out by heating the sawdust at 350°C for two

hours, using a stainless steel bowl (thermal cracking device); then, the charcoal is cooled to room temperature and, for the final carbonization, heated as the charcoal powder, using a muffle furnace after mixing it with KOH in a ratio (KOH:coal) of (2.5:1) by weight to a degree of 550°C for two hours. The mixture was then chilled and rinsed numerous times with distilled water until the pH reached 7. Then, it was immersed in a 10% hydrochloric acid solution and heated for two hours. Then, it is cooled to laboratory temperature and washed until the acidity of the wash water equal 7. It was heated thermally, using a solution of 0.1 N of KOH to transform it into charcoal with a basic character, and then, it was washed until the acidity of the washing water became 9, because the drug under study has an acidic character, after which the prepared activated charcoal was well dried, mechanically crushed, and isolated using molecular sieves before being preserved in sealed containers for further study.

2.3. Adsorbent (Chlorpheniramine)

TABLE 1. The drug used and some of its properties.

Drug name	Structure	Colour	λ_{max}, nm
Chlorpheniramine	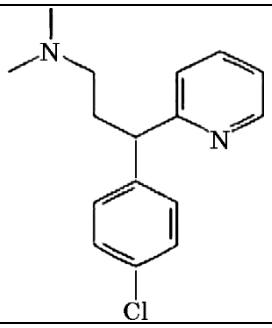	white	265

2.4. Determination of the Amount of Adsorbent

Both adsorption efficiency and capacity are used to express the amount of adsorbed substance by estimating the remaining amount in the solution. Because the drug under study was not coloured, the spectroscopic approach in the UV area, which is in the lower range (300 nm), was calculated. The amount of adsorbed material is defined by the difference between the initial and remaining concentrations in the solution. The calibration curve was used to determine these concentrations. The adsorbed material, adsorption efficiency, and adsorption capacity were determined using Eqs. (7)–(9):

$$A = \varepsilon bCl, \tag{7}$$

$$q_e = \frac{C_i - C_e}{m} V_L, \tag{8}$$

$$\text{Adsorption } [\%] = \frac{C_i - C_e}{C_i} \cdot 100\%. \tag{9}$$

Here, A is absorption, ε is absorption coefficient, C is concentration, l is cell width ($l = 1$ cm), C_i is initial concentration, and C_e is the remaining concentration, while $C_e - C_i$ represents the adsorbed concentration, which is symbolized by C_{ads}, and q_e represents the adsorption capacity for V_L—the volume of the drug solution in litres and m—the weight of the adsorbed material [g] (all concentrations are in the units [mg/L] ppm).

2.5. The Application of the Batch Method

All research on the influence of components on the adsorption process and its kinetic studies have been done, including using the study in a one-shot manner by altering certain variables and fixing others, as follow.

Drug solutions of varying strengths were made in hermetically sealed conical glass flasks under identical conditions. The adsorbent materials of commercial activated carbon and prepared activated carbon were then added to it, and it was shaken continuously at particular periods and rates (100 revolutions/minute), using a water bath vibrator after the temperature was adjusted.

2.6. Maximum Wavelength and the Calibration Curve

The highest wavelength (λ_{max}) was determined by recording the absorption spectrum of the drug solution with an appropriate concen-

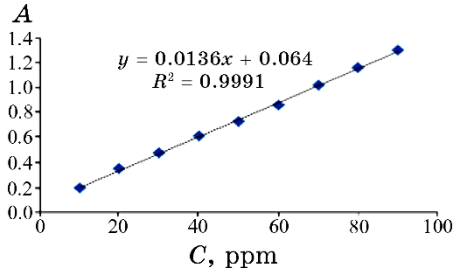

Fig. 1. Calibration curve for the drug theophylline [ppm].

tration and reading the highest absorption value, then, making a solution of the medication at various concentrations, assessing its absorption at those concentrations, and establishing a link between the intensity of absorption and the concentrations, to which the Beer–Lambert law must apply. The medication has a λ_{max} value of 265 nm.

3. RESULTS AND DISCUSSION

3.1. Adsorbent Material

To investigate the surface shape of the synthesized activated carbon (SAC), scanning electron microscopy (SEM) and x-ray diffraction (XRD) spectroscopy were used to assess the carbon model developed in this study, as shown in Fig. 2.

Scanning electron microscopy studies revealed a variance in the

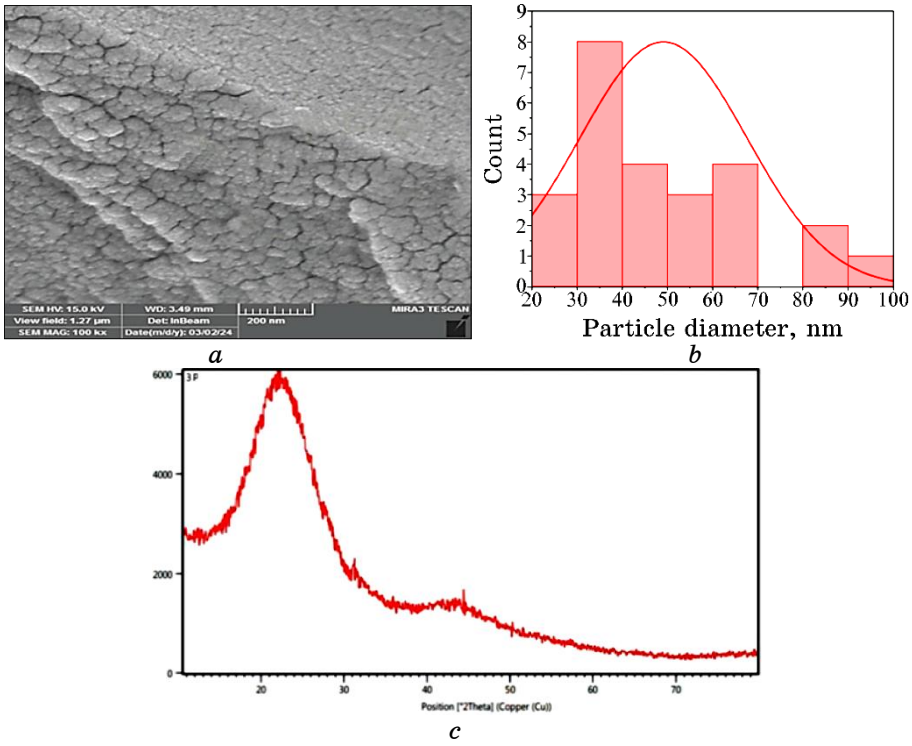

Fig. 2. *a*—SEM shapes of the prepared carbon (SAC) surfaces; *b*—statistics for the sizes of nanoparticles; *c*—XRD shapes of the prepared carbon (SAC) surfaces.

carbon nanoparticles' sizes (Fig. 2, *a*) with all of them being average nanosize of 20–100 nm, as shown in Fig. 2, *b*. Figure 2, *c* represent XRD utilized to analyze the crystalline morphologies of the carbon surface. This analysis found two bands at the positions (2Theta): first pick is between 20–30° and the other between 42–48°. This indicates the fabrication of nanosize particles.

3.2. The Effect of Adsorbent Weight

The results were obtained, when studying the effect of the amount of adsorbent at 60 min, a temperature of 25°C, a shaking speed of 100 rpm, and a volume of the drug solution of 25 ml (Tables 2–4).

From Table 2, the increasing amount of adsorbent material increases the rate of adsorption directly, while the adsorption capacity, on the contrary, is decreased due to the increase in the number of active sites on the surface of the adsorbent material to bind the

TABLE 2. Effect of the adsorbent on the efficiency and capacity of adsorption.

Adsorbent	C_i, mg/L	Adsorbent material, gm	C_e, mg/L	Adsorption, %	q_e, mg/g
SAC	120 ppm	0.01	72.922	39.231	117.695
		0.02	61.723	48.564	72.846
		0.04	46.779	61.017	45.763
		0.06	32.854	72.621	36.310
		0.08	23.841	80.132	30.049
		0.1	16.371	86.357	25.907

TABLE 3. Effect of concentration on the efficiency and capacity of adsorption.

Adsorbent	C_i, mg/L	C_e, mg/L	Adsorption, %	q_e, mg/g
SAC	70	1.321	98.112	17.169
	80	2.941	96.323	19.264
	90	6.189	93.123	20.952
	100	8.996	91.004	22.751
	110	12.412	88.716	24.397
	120	16.371	86.357	25.907
	140	25.071	82.092	28.732
	160	39.662	75.211	30.084
	180	60.982	66.121	29.754

TABLE 4. Effect of contact time on the efficiency and capacity of adsorption.

Adsorbent	t_{im}, min	C_e, mg/L	Adsorption, %	q_{et}, mg/g
SAC	10	63.727	46.894	14.068
	20	48.812	59.323	17.797
	30	35.878	70.101	21.030
	40	24.823	79.314	23.794
	50	19.185	84.012	25.203
	60	16.371	86.357	25.907
	70	15.626	86.978	26.093
	80	15.626	86.978	26.093

molecules of the material to be adsorbed, and this result is consistent with previous results of Refs. [16–18]. Therefore, we will limit our study in this research to the use of prepared coal because it is available in large quantities and, in addition, it also gave results similar to commercial coal.

3.3. The Effect of Initial Concentration

The results from studying the effect of the initial concentration of adsorption are shown in Table 3.

Table 3 shows that, as concentration increases, adsorption capacity does too, but adsorption efficiency (% of adsorption) declines. This could be attributed to the use of a defined amount of adsorbent with a specific number of active sites. It causes increased competition between drug molecules to bind to the active sites, resulting in a greater amount of the drug remaining in the solution after the equilibrium process, lowering adsorption efficiency, when calculated mathematically as the ratio of the amount of the adsorbed substance to the amount of the substance remaining in the solution.

3.4. Effect of Contact Time

Results were obtained, when studying the effect of time on the efficiency and capacity of adsorption at 25°C, the amount of charcoal prepared 0.08 gm, an initial concentration of 40 ppm, a shaking speed of 100 rpm, and a volume of the drug solution of 25 ml, as shown in Table 4.

The time effect data in this table demonstrate that the adsorption process is quite quick in the first few minutes and then gradually slows down until it reaches equilibrium, after that the adsorption

process is virtually constant [19]. The equilibrium state occurs, when the rate of binding of adsorbent (drug) molecules to the surface of the adsorbent material equals the rate, at which other molecules are released from the adsorbent surface into the solution. The study found that the substances studied reached a state of equilibrium between 70–80 minutes. This difference in adsorption rate occurs due to the presence of a large number of empty active sites on the surface of the adsorbent material. At the beginning of the adsorption process, they are suitable for binding to the adsorbent material. In addition, the concentration of the adsorbent material is higher at the beginning of the adsorption that favours the process of movement of the adsorbent molecules to the surface of the adsorbent. Over time, the number of adsorbents and the competition between the solution molecules for binding to these sites lead to a decrease in the rate of the adsorption process until the system reaches a state of equilibrium.

3.5. Effect of Temperature

The results obtained, when studying the effect of temperature, using the amount of adsorbent of 0.1 g, an initial concentration of 120 ppm, a time of 70 minutes, a shaking speed of 100 rpm, and a volume of the drug solution of 25 ml, are shown in Tables 5–7.

The results of the temperature effect in Table 5 show that increasing temperature leads to a decrease in the adsorption efficiency [in percentage] and adsorption capacity because increasing temperature accelerates the recovery process of the adsorbed molecules on the adsorbent surface into the solution (desorption) [20]. This is a result of the destruction of the binding forces between the adsorbent material and the adsorbent surface, indicating that the adsorption process is exothermic [21]. This indicates the physical nature of the adsorption in the system studied and it fully complies with the Le Chatelier's rule [19]. This is confirmed by the thermodynamic studies discussed in the following sections.

3.6. pH Effect

Results obtained, when studying the effect of acid function, are shown in Table 6. From Table 6 resulting from the effect of the acid function, we noticed that the capacity and efficiency of adsorption decrease clearly, when moving with the acid function from the acidic medium to the neutral and then basic ones. As found, the adsorption process occurs in different acidic functions and is least in the basic medium [22].

TABLE 5. Effect of temperature on the efficiency and capacity of adsorption.

Adsorbent	Temperature, K	C_e, mg/L	Adsorption, %	q_e, mg/g	K_e
SAC	288	15.295	87.254	26.176	6.845
	298	15.626	86.978	26.093	6.679
	308	17.859	85.117	25.535	5.719
	318	22.936	80.886	24.266	4.231
	328	28.784	76.013	22.804	3.168
	338	32.390	73.008	21.902	2.704

TABLE 6. Effect of acid function on the efficiency and capacity of adsorption.

Adsorbent	pH	C_e, mg/L	C_{ads}, mg/L	Adsorption, %	q_e, mg/g
SAC	2	9.572	110.428	92.023	27.607
	3	13.250	106.75	88.958	26.687
	4	14.959	105.041	87.534	26.260
	5.4	15.626	104.374	86.978	26.093
	7	19.870	100.130	83.441	25.032
	9	27.921	92.079	76.732	23.019

TABLE 7. Effect of solvent using ethanol on efficiency and capacity of adsorption, using natural acid function.

Adsorbent	Water:Ethanol,%	C_e, mg/L	C_{ads}, mg/L	Adsorption, %	q_e, mg/g
SAC	0:101	15.636	104.364	86.979	26.100
	10:90	21.343	98.657	82.213	24.664
	20:80	29.986	90.014	75.011	22.503
	30:70	41.875	78.125	65.104	19.531
	40:60	58.986	61.014	50.845	15.253
	50:50	73.174	46.826	39.021	11.706
	60:40	88.291	31.709	26.424	7.927
	70:30	107.877	12.123	10.102	3.030

3.7. Effect of Solvent

Results obtained, when studying the effect of the solvent, are shown in Table 7. These results regarding the effect of the solvent indicate that the efficiency and capacity of adsorption decrease with an increase in the percentage of ethanol, which is a decrease in the

percentage of water compared to an increase in the percentage of ethanol in the mixture, which is a decrease in the dielectric constant of the solvent, as it is known that water is the most valuable solvent with its dielectric constant, which is of 80 that is higher than for ethanol. Therefore, combining it with ethanol generates solvents with a lower dielectric constant [23]. As the dielectric constant of the solvent increases, this one does the solute tendency to migrate to the surface of the adsorbent material, as opposed to molecular interactions of the solute–solute and solvent–solute types. As a result, we find that, as the solvent dielectric constant increases, its adsorption efficiency so does too.

3.8. Calculating of Thermodynamic Functions

Thermodynamic functions are one of the most important variables to consider, when studying adsorption processes. They describe the characteristics of the system being studied as well as the factors, which influence that system and the course of the adsorption process. In addition, they can reveal the type of molecular interactions, which may occur during the adsorption process and play an important role in assessing its effectiveness. The heat of adsorption can be calculated using the van't Hoff equation, which shows the relationship between temperature and the equilibrium constant:

$$K_e = K_0 e^{-\frac{\Delta H}{RT}}; \tag{10}$$

here, ΔH represents the heat of adsorption, K_e represents the equilibrium constant for adsorption, and K_0 represents a constant value. Taking ln for both sides, we get the following form:

$$\ln K_e = \ln K_0 - \frac{\Delta H}{RT}. \tag{11}$$

The value of ΔH can be found by drawing the relationship between $\ln K_e$ *versus* the reciprocal of temperature $(1/T)$, which gives a straight line with a slope equal to $(-\Delta H/R)$, and by knowing the value of the equilibrium constant for adsorption, which can be found from the ratio between concentrations of the adsorbed material remaining in the solution:

$$K_e = \frac{C_{ads}[\text{mg/L}]}{C_e[\text{mg/L}]}. \tag{12}$$

It is possible to find the value of ΔH and then the other thermodynamic functions ΔS^0, ΔG^0 through the following equations:

$$\Delta G^0 = -RT\ln K_e, \tag{13}$$

$$\Delta G^0 = \Delta H - T\Delta S^0, \tag{14}$$

$$\Delta S^0 = \frac{\Delta H - \Delta G^0}{T}. \tag{15}$$

The ΔG value indicates the change in standard free energy at each stage of adsorption, while ΔG^0 represents the zero value and free energy, if the equilibrium process remains constant. The ΔS^0 value represents the system condition at each adsorption step [24, 25].

In Figure 3, the practical data of the studied system at equilibrium are subject to the linear relationship between $\ln K_e$ and $1/T$ using the van't Hoff Eq. (11), which is inferred through the values of the correlation coefficient (R^2) for the straight line, and when looking at the values of the thermodynamic functions as well as the values of the equilibrium constants, which were clarified and listed in Table 8. It is noted, they are changed as follow.

1. The values of the equilibrium constant K_e decrease with increasing temperature for the drug that is consistent with that was found from studying the effect of temperature, namely, the efficiency of adsorption decreases with increasing temperature, indicating that

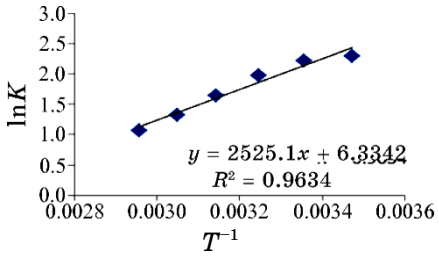

Fig. 3. Thermodynamic functions for drug adsorption.

TABLE 8. Equilibrium constants and thermodynamic functions at equilibrium.

Adsorbent material	Temperature, K	K_e	ΔG^0, kJ·mol^{-1}	ΔH, kJ·mol^{-1}	ΔS^0, J·mol^{-1}·K^{-1}
SAC	289	6.845	–4.605	–16.452	–41.135
	297	6.679	–4.704		–39.422
	308	5.719	–4.465		–38.918
	318	4.231	–3.813		–39.745
	328	3.168	–3.144		–40.573
	338	2.704	–2.795		–40.405

the forces responsible for the adsorption process are physical forces, as the increase in temperature leads to breakdown of them. Then, the adsorbed molecules return to the solution, and this statement is firmly supported by the value of ΔH (–16.452 kJ·mol^{-1}).
2. Enthalpy change ΔH calculated was of a negative sign that indicates that the adsorption process is heat emitting, while its values indicate that the forces responsible for the adsorption process are van der Waals forces, as the value obtained is less than 40 kJ/mol, which is within the energy range of physical bonds [26].
3. The negative values of ΔS^0 give an indication of the state of order in the studied system, and its values are within the certain range and are close with each other (at all temperatures). This supports that the system is of a physical nature, and that the role of entropy change is limited.

These results are supported by the values of the change in free energy ΔG^0, as its values indicate a decrease in the spontaneity of adsorption with the increase in temperature.

3.9. Adsorption Isotherms

3.9.1. Freundlich's Isotherm

By applying Eq. (1) for this isotherm to the practical data for adsorption, by drawing the graphical relationship between $\ln q_e$ *versus* $\ln C_e$, and through it, the values of the Freundlich's constants (K_F, n) were calculated from the slope (n) and the cross-section (K_F) of the straight line, as shown in Fig. 4.

The results listed in Table 9 indicate that the Freundlich's isotherm equation applies to the practical data of the well-studied adsorption system through the values of the correlation coefficient close to one. The values of n within the range between 1–10 also indicate that the adsorption system is of type preferably governed by physical forces [27, 28], and this is consistent with that shown by the values of ΔH, while the values of K_F are related to the adsorption capacity, and its high values indicate the efficiency of adsorption [29].

3.9.2. Langmuir's Isotherm

When applying Eq. (2) to this model by drawing the linear relationship between C_e/q_e *versus* C_e, it gives a slope equal to $1/Q_{\max}$ and an intercept equal to $b^{-1}Q_{\max}$ [30], as shown in Fig. 5.

Figure 5 shows that excellent linear relationships were obtained through high correlation-coefficient value of 0.9935, and thus, a

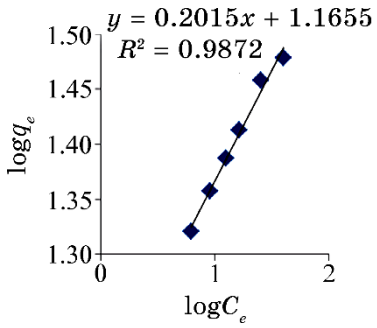

Fig. 4. Application of Freundlich's isotherm to practical data for adsorption of the studied drug.

TABLE 9. Freundlich's constants (K_F, n) and correlation coefficient obtained by applying them to practical adsorption data.

n	K_F	R^2
4.962	14.639	0.9872

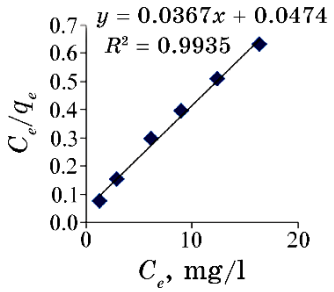

Fig. 5. Application of the Langmuir's isotherm to experimental drug adsorption data.

TABLE 10. Values of the Langmuir's constants (Q_{max}, b) and the correlation coefficient.

Q_{max}, mg/g	b, L/mg	R^2
27.247	1.344	0.9935

conclusion can be made that the practical results of adsorption for the systems under study showed greater agreement with this isotherm in describing the adsorption process than their application to the Freundlich's isotherm.

The value of the Langmuir's constant b, which represents the

bond strength between the molecules of the adsorbed substance on the adsorbent surface, is small. This means that the bond strength is weak that indicates that the adsorption is physical, and this supports the value of ΔH obtained from the thermodynamic study also noticing that the value of the maximum theoretical adsorption capacity (Q_{max}) does not depend on the nature of the adsorbent material alone, but rather on other matters related to the nature of the adsorption system, including the nature of the adsorbed material and the aggregates associated with it, the surface area, the geometric shape, the method of its attachment to the adsorbed surface, as well as the interactions between the adsorbed molecules on the surface and the attacking ones, to compete for the remaining sites and between them on the other hand [31].

4. KINETIC STUDY

4.1. Pseudo-First Order Equation

The pseudo-first order equation model, Eq. (3), was applied by drawing the relationship between $\ln(q_e - q_t)$ *versus* t—the time per minute to obtain a linear relationship with the magnitude of its slope $-k_1$ and its intercept $\ln q_e$, and, through it, values of q_e and k_1 can be found.

The shape and results obtained are shown in Fig. 6 and listed in Table 11.

Comparing the practical or experimental adsorption capacity with their theoretical values, shown in Table 11, it was noted that these

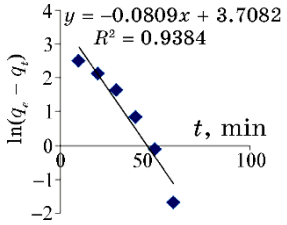

Fig. 6. Application of the pseudo-first order model to experimental drug adsorption data.

TABLE 11. Practical and theoretical pseudo-first-order velocity constants, adsorption capacity and the correlation coefficient.

$q_{e(exp)}$, mg/g	$q_{e(calc)}$, mg/g	k_1, min^{-1}	R^2
26.093	28.780	0.0809	0.9384

values are not identical and not close to each other, and the values of the correlation coefficient (R^2) are not good, as it can explain this situation as follow. It is the possibility of a kinetic application of this model at a certain stage of the adsorption process, and Langmuir's Eq. (3) cannot be applied to a large extent with practical values of adsorption because the theoretical basis assumed by this equation deviates from the practical values and the diffusion of drug molecules through the pores of activated charcoal, the initial concentration of the drug cannot be in a linear relationship with the rate of adsorption speed, despite the linear relationship given by the application of that equation.

These results represent the initial stage of the adsorption process and not at all time periods of the adsorption process; the process is fast in its beginning. In general, it can be concluded that the application of practical values for adsorption does not fully agree with the theoretical basis of the Lagergren equation for the adsorption system [32].

4.2. Pseudo-Second Order Equation

Applying pseudo-second order model to practical adsorption data by plotting the relationship between t/q_t *versus* time, it is also possible to use adsorption rate constant k_2 to find the initial pseudo-second-order adsorption speed (h) through Eq. (5).

The application of the pseudo-second order model gave an excellent linear relationship, which indicates that a high correlation coefficient was obtained, as shown in Fig. 7, where the condition of

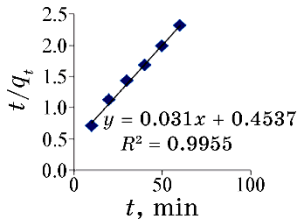

Fig. 7. Application of the pseudo-second order to experimental drug adsorption data.

TABLE 12. Rate constant and the practical and theoretical pseudo-second order adsorption capacity and correlation coefficient.

$Q_{e(\text{exp})}$, mg/g	$q_{e(\text{calc})}$, mg/g	k_2, g·mg^{-1}·min^{-1}	h, mg·g^{-1}·min^{-1}	R^2
26.093	32.258	0.00211	1.436	0.9955

this model matching the adsorption kinetics to the practical results of adsorption was achieved through the convergence of the practical values of the adsorption capacity at equilibrium $q_{e(\exp)}$ with the values of $q_{e(\text{calc})}$ calculated theoretically from the intersection of the straight line of the graph. For this reason, it can be said that the practical results of adsorption are subject to the false second-order model. Within the specified time period for the adsorption process, one of the reasons [32] why the practical results of adsorption are not subject to this model may be the presence of influencing forces, which determine the rate of adsorption, such as the concentration of the adsorbent and the nature of the adsorption process, in addition to the path taken by the adsorbed-solution molecules in the process of their transfer from the solution to the surface of the adsorbent and their spread through its internal pores. As for the values of h, which is called the initial rate of adsorption, the results calculated for it and shown in Table 12 indicate that, at the higher adsorption efficiency of the drug, the surface of the adsorbed material will be occupied by the molecules of the adsorbed material faster that leads to a greater slowdown of the speed of the adsorption process. This is consistent with that observed, when studying the effect of time on adsorption efficiency [33].

4.3. Intra-Particle Diffusion Model

The implicit particle-diffusion model is applied to the practical data for adsorption by applying Eq. (6) by drawing the relationship between the values of q_t *versus* the square root of time. The value of C gives evidence of the thickness of the outer layer of the solution boundaries and its effect, as a high value of C indicates that this class has a greater influence [34].

The mechanics of the adsorption process can occur in three steps: first, the transfer of the adsorbed molecule from its location in the solution to the surface of the adsorbent after overcoming all the interfacial forces, which hinder its movement in the solvent; its association with the active sites on the adsorbent surface; and finally, its spread through the internal pores of the adsorbent surface.

The mechanism of implicit molecular diffusion will be the only mechanism guiding the adsorption process, only when drawing the relationship between q_t *versus* $t^{1/2}$ gives a straight line passing through the origin. Since this does not happen, this indicates that the process of implicit molecular diffusion plays an important role in the process of removing the drug from its aqueous solutions using activated charcoal. However, the experimental results suggest that it is not the only mechanism controlling the drug adsorption, as shown in the results obtained in Fig. 8 and Table 13.

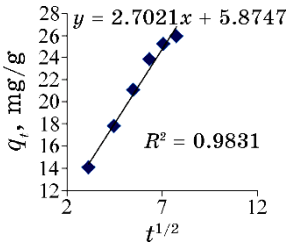

Fig. 8. Application of the implicit molecular-diffusion model to practical drug adsorption data.

TABLE 13. Values of implicit molecular-diffusion constants and correlation coefficient.

C_i, mg/L	K_{diff}, mg·g^{-1}·min$^{-1/2}$	C, mg/g	R^2
120	2.7021	5.8747	0.9831

5. CONCLUSIONS

Dry or wet sawdust, which is the waste of wood industries, most importantly furniture for homes and government institutions, causes environmental pollution and detracts from the beauty and cleanliness of nature. Therefore, through this study, we tried to convert it into a material that benefits the general economy of any country by producing activated nanocarbon (of 20–100 nm) compounds in the form of industrial activated charcoal. Comparison of the two carbons showed that the nanocarbon prepared in this study was highly efficient in removing pharmaceutical pollutants, especially, expired drugs, which contain the substance (chlorpheniramine), more than the commercial charcoal used in the markets and prepared by traditional methods.

ACKNOWLEDGEMENTS

Authors would like to thank the University of Mosul, College of Science, as well as Mr. Faris M. Alhamadany (MSc. Phys., University of Newcastle (U.K.), 'Work in Nineveh Medicine College, Iraq') and Mr. Alaa Mohammed (New York Times, correspondent) for editing and reviser of the language.

REFERENCES

1. V. Pravdić, *Science of the Total Environment Journal*, **171**, No. 3: 265

(1995); https://doi.org/10.1016/0048-9697(95)04694-8
2. J. P. Sumpter, Journal *of Physical and Engineering Sciences*, **367**, No. 1904: 3877 (2009); https://doi.org/10.1098/rsta.2009.0106
3. M. T. Khan, I. A. Shah, I. Ihsanullah, M. Naushad, S. Ali, S. H. A. Shah, and A. W. Mohammad, *Journal of Water Process Engineering*, **41**, No. 8: 101990 (2021); https://doi.org/10.1016/j.jwpe.2021.101990
4. A. S. Khan, A. Anavkar, A. Ali, N. Patel, and H. Alim, *Biosciences Biotechnology Research Asia*, **18**, No. 1: 9 (2021); http://dx.doi.org/10.13005/bbra/2893
5. M. A. Al-Ghouti and D. A. Da'ana, *Journal of Hazardous Materials*, **393**, No. 2: 122383 (2020); https://doi.org/10.1016/j.jhazmat.2020.122383
6. A. L. Myers and P. A. Monson, *Adsorption Journal*, **20**: 3591 (2014); https://doi.org/10.1007/s10450-014-9604-1
7. C. Moreno-Castilla, *Carbon Journal*, **42**, No. 1: 83 (2004); https://doi.org/10.1016/j.carbon.2003.09.022
8. L. X. Liu and J. D. Litster, *Powder Technology Journal*, **74**, No. 3: 259 (1993); https://doi.org/10.1016/0032-5910(93)85034-7
9. G. G. Granqvist and R. A. Buhrman, *Journal of Applied Physics*, **47**, No. 5: 2200 (1976); https://doi.org/10.1063/1.322870
10. R. L. Tseng, F. C. Wu, and R. S. Juang, *Journal of the Taiwan Institute of Chemical Engineers*, **41**, No. 6: 661 (2010); https://doi.org/10.1016/j.jtice.2010.01.014
11. V. K. Gupta, S. Agarwal, A. K. Bharti, and H. Sadegh, *Journal of Molecular Liquids*, **230**: 667 (2017); https://doi.org/10.1016/j.molliq.2017.01.083
12. F. Rassaei, *Communications in Soil Science and Plant Analysis*, **54**, No. 15: 2059 (2023); https://doi.org/10.1080/00103624.2023.2211116
13. S. Svilović, D. Rušić, and A. Bašić, *Desalination*, **259**, Nos. 1–3: 71 (2010); https://doi.org/10.1016/j.desal.2010.04.033
14. P. S. Pauletto, G. L. Dotto, and N. P. G. Salau, *Chemical Engineering Research and Design*, **157**: 182 (2020); https://doi.org/10.1016/j.cherd.2020.02.031
15. E. Asuquo, A. Martin, P. Nzerem, F. Siperstein, and X. Fan, *Journal of Environmental Chemical Engineering*, **5**, No. 1: 679 (2017); https://doi.org/10.1016/j.jece.2016.12.043
16. S. De Gisi, G. Lofrano, M. Grassi, and M. Notarnicola, *Sustainable Materials and Technologies*, **9**, No. 5: 10 (2016); https://doi.org/10.1016/j.susmat.2016.06.002
17. M. A. Al-Ghouti, J. Li, Y. Salamh, N. Al-Laqtah, G. Walker, and M. N. Ahmad, *Journal of Hazardous Materials*, **176**, No. 1: 10 (2010); https://doi.org/10.1016/j.jhazmat.2009.11.059
18. X. Li, L. Zhang, Z. Yang, P. Wang, Y. Yan, and J. Ran, *Separation and Purification Technology*, **235**: 116213 (2020); https://doi.org/10.1016/j.seppur.2019.116213
19. Mustafa T. Yagub, Tushar Kanti Sen, and H. M. Ang, *Water, Air & Soil Pollution*, **223**: 5267 (2012); https://doi.org/10.1007/s11270-012-1277-3
20. G. T. Tee, X. Y. Gok, and W. F. Yong, *Environmental Research*, **212**: 113248 (2022); https://doi.org/10.1016/j.envres.2022.113248
21. M. K. Uddin and A. Nasar, *Scientific Reports*, **10**, No. 1: 7983 (2020); https://doi.org/10.1038/s41598-020-64745-3

22. V. Fierro, V. Torné-Fernández, D. Montané, and A. Celzard, *Microporous and Mesoporous Materials*, **111**, No. 3: 276 (2008); https://doi.org/10.1016/j.micromeso.2007.08.002
23. F. Fanari, G. Muntoni, C. Dachena, R. Carta, and F. Desogus, *Energies*, **13**, No. 18: 4861 (2020); https://doi.org/10.3390/en13184861
24. É. C. Lima, M. H. Dehghani, A. Guleria, F. Sher, R. R. Karri, G. L. Dotto, and H. N. Tran, *Green Technologies for the Defluoridation of Water* (Elsevier: 2021), pp. 41–88; https://doi.org/10.1016/B978-0-323-85768-0.00004-X
25. X. You, R. Zhou, Y. Zhu, D. Bu, and D. Cheng, *Journal of Hazardous Materials*, **430**: 128445 (2022); https://doi.org/10.1016/j.jhazmat.2022.128445
26. A. Kokalj, *Corrosion Science*, **196**: 109939 (2022); https://doi.org/10.1016/j.corsci.2021.109939
27. P. Pourhakkak, A. Taghizadeh, M. Taghizadeh, M. Ghaedi, and S. Haghdoust, *Interface Science and Technology* (Elsevier: 2021), vol. **33**, p. 1; https://doi.org/10.1016/B978-0-12-818805-7.00001-1
28. R. S. Liu, X. D. Shi, C. T. Wang, Y. Z. Gao, S. Xu, G. P. Hao, and A. H. Lu, *Chem. Sus. Chem.*, **14**, No. 6: 1428 (2021); https://doi.org/10.1002/cssc.202002677
29. M. Y. Choi, C. G. Lee, Y. M. Yoon, and S. J. Park, *Applied Organometallic Chemistry*, **7**, No. 3: 672 (2024); https://doi.org/10.1002/aoc.7672
30. S. T. Al-Asadi, F. F. Al-Qaim, H. F. S. Al-Saedi, I. F. Deyab, H. Kamyab, and S. Chelliapan, *Environmental Monitoring and Assessment*, **195**, No. 6: 676 (2023); https://doi.org/10.1007/s10661-023-11334-2
31. S, Gao, S. Zhao, X. Tang, Y. Wang, and H. Yi, *Fuel*, **359**: 130394 (2024); https://doi.org/10.1016/j.fuel.2023.130394
32. X. Zhu, Z. Wang, J. Ren, N. AlMasoud, Z. M. S. El-Bahy, T. Alomar, and X. Guo, *Advanced Composites and Hybrid Materials*, **6**, No. 5: 169 (2023); https://doi.org/10.1007/s42114-023-00731-3
33. M. S. Kazemi and A. Sobhani, *Arabian Journal of Chemistry*, **16**, No. 6: 104754 (2023); https://doi.org/10.1016/j.arabjc.2023.104754